

# Measurements of Flows with Tangential Injection and Comparison with Prediction Methods

R.J. Kind\* and K. Gooden†  
*Carleton University, Ottawa, Ontario, Canada*  
 and  
 F.A. Dvorak‡  
*Analytical Methods, Inc., Bellevue, Wash.*

Experiments involving boundary-layer control by tangential injection are described. Velocity profiles were measured in 18 different two-dimensional flows over plane and strongly curved surfaces with a variety of adverse pressure gradients. The data include a wide variety of velocity-profile types. Data for six representative flows are presented in the paper. The data are compared with two prediction methods.

## Nomenclature

$C_\mu$	= injection momentum coefficient, $(\dot{m}^2 / \rho_j t) / \frac{1}{2} \rho_\infty U_\infty^2 d$
$C_p$	= static pressure coefficient, $(p - p_\infty) / \frac{1}{2} \rho_\infty U_\infty^2$
$d$	= cylinder diameter
$\dot{m}$	= mass flux from injection slot, per unit span
$p$	= static pressure
$P_0$	= total pressure in plenum chamber
$P_t$	= maximum total pressure in wall jet
$t$	= thickness of injection slot
$u$	= local velocity of flow (see Fig. 2)
$U$	= freestream velocity
$x$	= streamwise coordinate along plane wall (see Fig. 2)
$y$	= coordinate normal to surface (see Fig. 2)
$\theta$	= angular coordinate (see Fig. 2)
$\rho$	= fluid density

## Subscripts

$c$	= flow on cylinder
$J$	= conditions at exit of injection slot
$w$	= flow on plane wall
$\infty$	= conditions in undisturbed freestream

## I. Introduction

TANGENTIAL injection is a familiar method of providing boundary-layer control to delay or prevent flow separation. An application of much current interest is "circulation control."<sup>1</sup> Circulation-control airfoils have a well rounded trailing edge, and tangential injection is used to move the upper-surface flow separation point around this trailing edge, thus producing high values of circulation and lift. The lift developed by a circulation-control airfoil can be varied rapidly with relative ease; this and other advantages make the concept particularly attractive for use on rotorcraft.<sup>1,2</sup> High lift coefficients can also be achieved together with low effective drag, making the scheme attractive for fixed-wing STOL aircraft as well.<sup>3</sup>

The flowfield associated with applications of tangential injection is relatively complex since it involves the mixing of a turbulent wall jet with a turbulent boundary layer (the up-

stream boundary layer) in a strong adverse pressure gradient, and, in the case of circulation control, on a highly curved surface. The complexity of the flowfield and the wide range of possible flow behaviors imply that a wide variety of experimental data is required to guide development and to enable assessment of prediction methods for tangential injection. The main objective of the present work was to provide additional flowfield data suitable for these purposes, especially data representative of circulation-control flows. At present the results available are very limited. A number of flowfield measurements are available for plane two-dimensional wall jets developing in uniform flows or in adverse pressure gradients with a negligible upstream boundary layer; see for example Refs. 4-6. Irwin<sup>7</sup> has performed measurements for a number of cases where the upstream boundary-layer thickness is appreciable, as has McGahan.<sup>8</sup> Several sets of flowfield data are available for wall jets with strong streamwise curvature in still air, for example Refs. 9-11. However, the only previous measurements typical of flow downstream of an injection slot at the knee of a highly deflected flap or on a circulation control airfoil (i.e., strong adverse pressure gradient, a substantial upstream boundary layer, and strong streamwise curvature) are those of Ref. 12.

In this paper new experimental results are presented and compared with the two most recent prediction methods<sup>13,14</sup> that are suitable for strongly curved flows with tangential injection. The comparisons are presented simply to enable the capabilities of the methods to be further assessed in the light of the new data.

## II. Apparatus and Experimental Methods

A sketch of the apparatus and the overall flowfield is shown in Fig. 1. Basically the apparatus consists of a 12.7-cm-diam cylinder mounted in close proximity to one sidewall of a 50.8 × 76 cm low-speed wind tunnel. Tangential injection

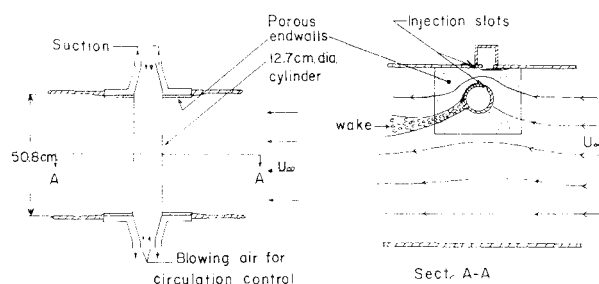


Fig. 1 Sketch of apparatus and flowfield.

Received Aug. 17, 1978, revision received Feb. 5, 1979. Copyright © American Institute of Aeronautics and Astronautics, Inc., 1979. All rights reserved.

Index categories: Jets, Wakes, and Viscid-Inviscid Flow Interactions; Aerodynamics; Boundary Layers and Convective Heat Transfer—Turbulent.

\*Associate Professor of Engineering, Member AIAA.

†Graduate Student. Now at Ontario Hydro, Toronto, Ontario.

‡President. Member AIAA.

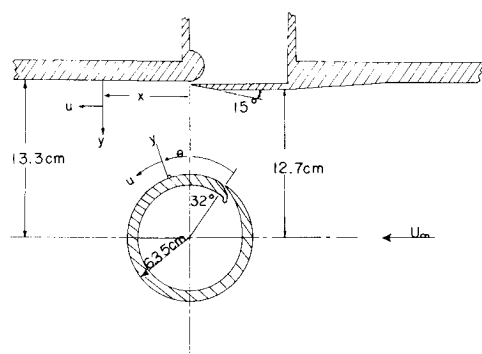


Fig. 2 Detailed geometry of apparatus and coordinate system.

Table 1 Flow conditions

Flow designation	Surface	$C_{\mu_w}$	$C_{\mu_c}$
A	Plane wall	0.22	0.30
B	Plane wall	0.15	0.30
C	Plane wall	0.07	0.30
D	Cylinder	0.07	0.30
E	Cylinder	0.07	0.20
F	Cylinder	0.07	0.10

from a slot in the surface of the cylinder provides circulation control<sup>1</sup> on the cylinder, thus enabling variation of the static pressure distribution on the cylinder itself and of the pressure distribution that the cylinder impresses on the side wall of the wind tunnel. Another slot in the side wall near the cylinder permits the use of tangential injection on the side wall as well. Suction is applied to the porous end walls to suppress the strong end effects which would otherwise occur when circulation control is applied to the cylinder. The apparatus thus provides tangential-injection flows on both a plane wall and on a curved wall. A wide variety of static pressure gradients can be produced simply by adjusting the momentum flux from the slots in the cylinder and in the side wall.

Figure 2 shows the detailed geometry of the apparatus as used throughout the experiments reported in this paper; it also defines the coordinate system used for presentation of the results. The cylinder was pressure-tapped around its circumference at the midspan position. The plane wall was fitted with a row of pressure tappings along the midspan position and with spanwise rows of taps at  $x = 18$  cm and  $x = 28$  cm to enable two-dimensionality checks.

The plenum chamber for each injection slot was supplied with blowing air from both ends. The mass flow rate of this air was determined by means of orifice plates. The injection slot in the plane wall had a mean thickness of 0.94 mm while that in the cylinder has a mean thickness of 0.91 mm. These mean slot thicknesses were determined by dividing the volume flow rate supplied to each slot in still-air conditions by the velocity corresponding to isentropic expansion from plenum pressure to ambient pressure. For both slots, the thickness varied less than 0.025 mm across the central 35 cm of the slot and less than 0.05 mm across the entire 49.5-cm span of the slots. The lip of the slot in the plane wall was essentially sharp while that on the cylinder was squared off to a thickness of 0.25 mm.

Mean velocity profiles were measured at the slot exits and at various positions downstream of the slots on both the plane wall and circular cylinder. A linearized constant temperature hot-wire anemometer was used for this purpose. The nominal wind-tunnel speed was 21 m/s in all runs. The momentum coefficient  $C_{\mu}$  (based on cylinder diameter) ranged from 0.10 to 0.30 for the cylinder and from 0.07 to 0.22 for the plane wall. The momentum flux from each slot was taken to be

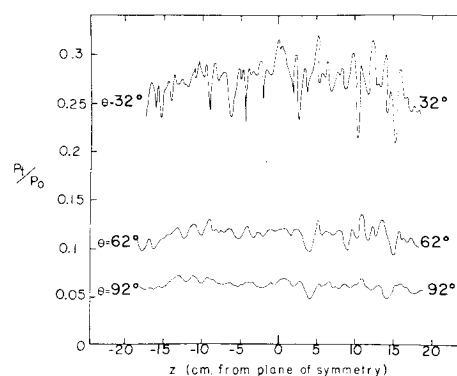


Fig. 3 Spanwise distribution of maximum total pressure in wall jet on cylinder in still air.

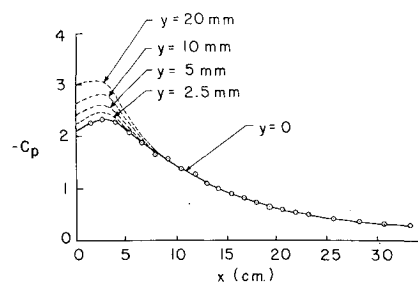


Fig. 4 Static pressure distribution in flows A, B, and C.

$\dot{m}^2 / \rho_f t$ , where  $\dot{m}$  is the mass flux per unit span,  $\rho_f$  is the density of the injection air, and  $t$  is the mean thickness of the slot, determined as outlined earlier.

The suction applied to the porous end plates was sufficient to remove at least two times the momentum thickness of the end-plate boundary layer. Strong positive suction prevailed all over the porous end plates under all conditions.

### III. Results and Discussion

#### A. Flow Quality Checks

The two-dimensionality of the flow issuing from the injection slots was examined by measuring the spanwise distribution of maximum total pressure  $P_t$  and of Preston tube readings in still-air conditions. Downstream of the slot on the plane wall, spanwise nonuniformity of the measured quantities was always within  $\pm 2.5\%$  over the central 30 cm of the span. On the cylinder, however, there were somewhat random short wavelength fluctuations of these quantities across the span, as illustrated in Fig. 3. This occurred despite the fact that the slot geometry and the total pressure at the slot exit were essentially uniform and despite the fact that the surface of the cylinder was smooth. This type of behavior has been observed before<sup>10-12</sup> and is thought to be an unavoidable consequence of the inherent instability of the flow in the outer region of a wall jet with convex curvature. The pattern of the fluctuations is essentially steady with time. The fluctuations are reduced, but not eliminated, by the presence of a freestream flow outside the curved wall jet. The static pressure distribution and the growth rate for the wall jet on the circular cylinder in still air agreed well with the results of other investigators.<sup>15,16</sup>

In the wind tunnel, two-dimensionality of the flow was checked by tuft studies, static pressure measurements, and velocity profile measurements. An array of fine tufts attached to the surface showed good alignment with the nominal freestream direction over the central 40 cm of the flow span under all conditions of interest, provided that the end-plate suction was operating. A very distinct deterioration of the flow quality was indicated when suction was discontinued. For  $C_{\mu_c} = 0.30$ ,  $C_{\mu_w} = 0$ , a condition in which end effects

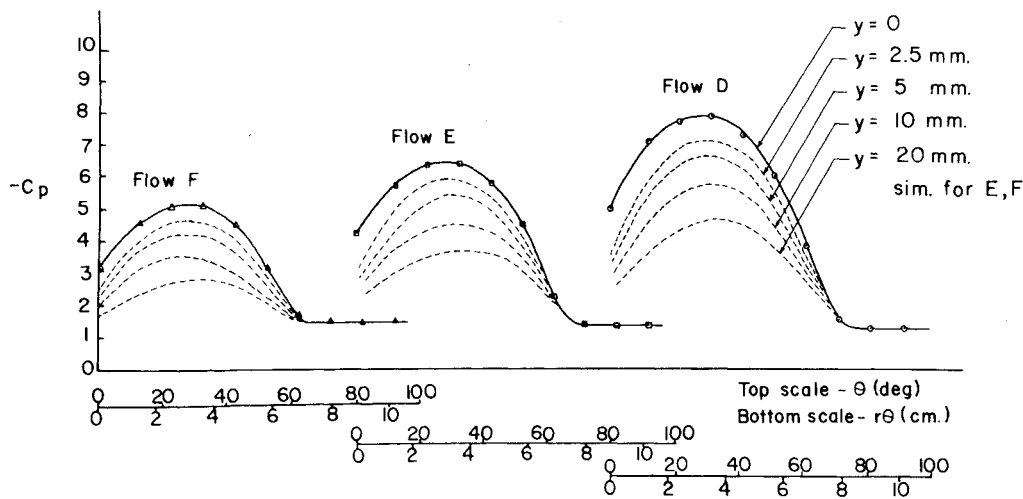


Fig. 5 Static pressure distribution in flows D, E, and F.

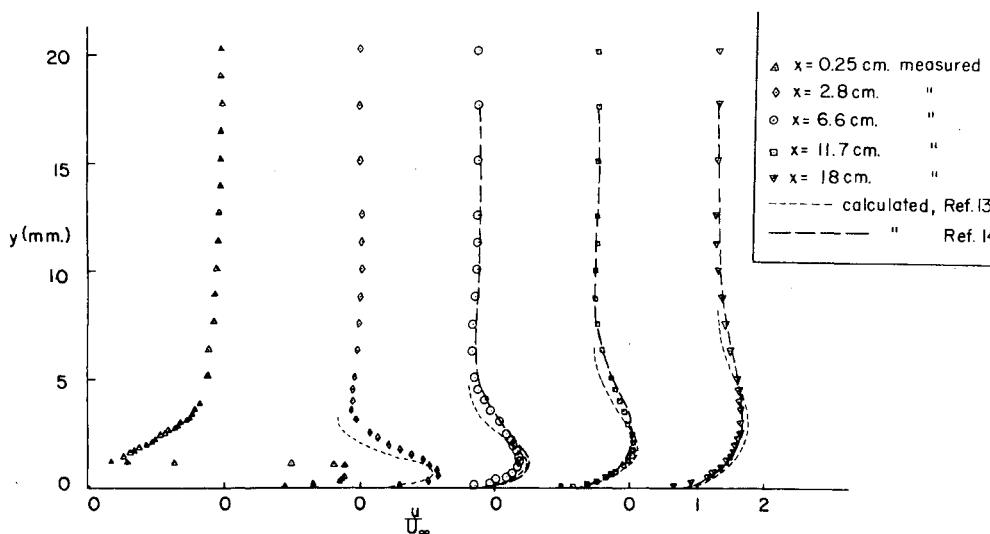


Fig. 6 Measured and calculated velocity profiles for flow A.

would tend to be particularly severe, the static pressure coefficient on the plane wall was constant within  $\pm 0.015$  at  $x = 18$  cm and  $x = 28$  cm over the central 35 cm of the flow. Velocity profiles were measured 14-cm above and below the plane of symmetry at several downstream stations for flows A, C, D, and F (see Table 1) and also for the condition  $C_{\mu c} = 0.30$ ,  $C_{\mu w} = 0$ . Except for  $x > 18$  cm on the plane wall, all velocities both within and outside the shear flow were within 2% of the corresponding velocities in the plane of symmetry. As discussed by Guitton and Newman,<sup>11</sup> such small departures from two-dimensionality are not expected to have a significant effect on measured mean velocity and turbulent shear stress distributions; however, poor results will be obtained for shear stresses calculated by using the mean velocity data in the equations of motion. Beyond  $x = 18$  cm on the plane wall, the spanwise variation of mean velocity increased, becoming  $\pm 10\%$  at  $x = 28$  cm. Therefore, no velocity profiles are presented for  $x > 18$  cm.

## B. Experimental Results

Velocity profiles on the plane wall and on the cylinder were measured for nine different combinations of  $C_{\mu w}$  and  $C_{\mu c}$ , the plane-wall and cylinder momentum coefficients, respectively. Thus, data for 18 different flow developments were obtained; the results for six representative cases are presented in this paper. Table 1 summarizes the flow conditions for each of these flows which are designated by the letters A to F. Figure 4 shows the static pressure distribution along the plane wall for flows A, B, and C. The static pressure

distribution is virtually identical for all three cases because none of these flows separated from the plane wall and the cylinder momentum coefficient is the same in all three cases; the flowfield outside the wall jet is thus the same for all three cases, and the wall jets, being plane, do not significantly affect the pressure distributions. The static pressure distributions on the surface of the cylinder are shown in Fig. 5 for flows D, E, and F. It can be seen that the adverse pressure gradient along flows D, E, and F is much stronger than that along flows A, B, and C.

Figures 6-8 show the velocity profiles measured on the plane wall for flows A, B, and C. These three flows clearly show a velocity minimum in the profiles near the slot, indicating that the fluid from the upstream boundary layer has not yet been completely entrained into the wall jet. In flows A and B, where the momentum coefficient  $C_{\mu w}$  is relatively large, the wall jet eventually dominates the flow, completely entraining the fluid from the upstream boundary layer and thus eliminating the velocity minimum in the profiles. In flow C, on the other hand, the momentum issuing from the slot is relatively small and the upstream boundary-layer fluid eventually dominates the flow; both the velocity maximum and the velocity minimum eventually disappear and the flow assumes the character of a more or less conventional turbulent boundary layer. At the measuring station the velocity profile of this boundary layer is similar to that of an ordinary turbulent boundary layer in an adverse pressure gradient, but of course its turbulent structure would be rather different due to its unusual recent history. None of the flows on the plane wall underwent separation.

Fig. 7 Measured and calculated velocity profiles for flow B.

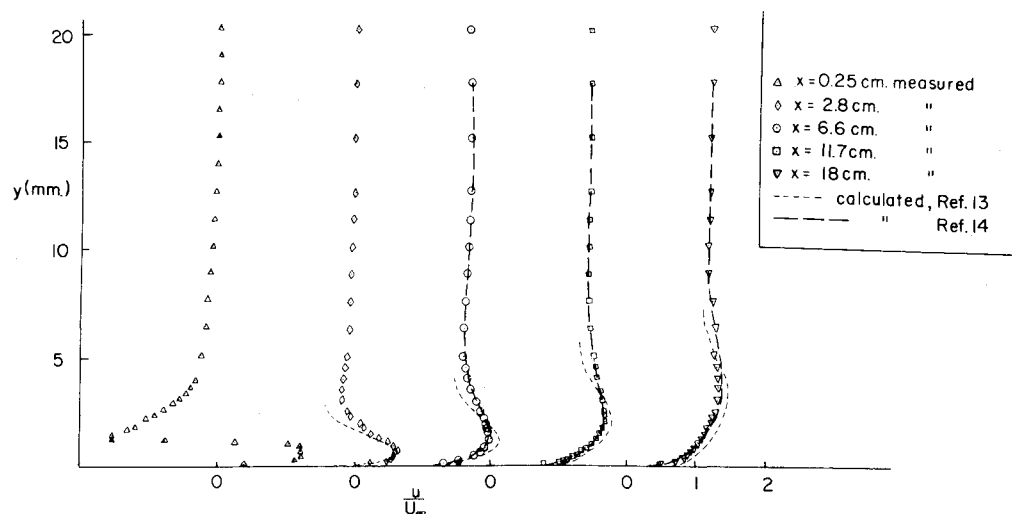


Fig. 8 Measured and calculated velocity profiles for flow C.

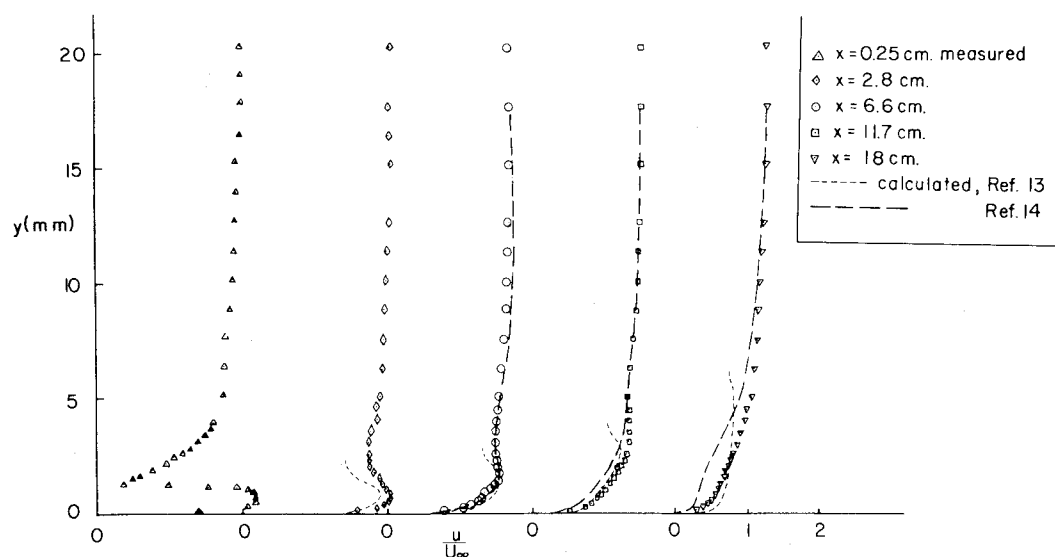
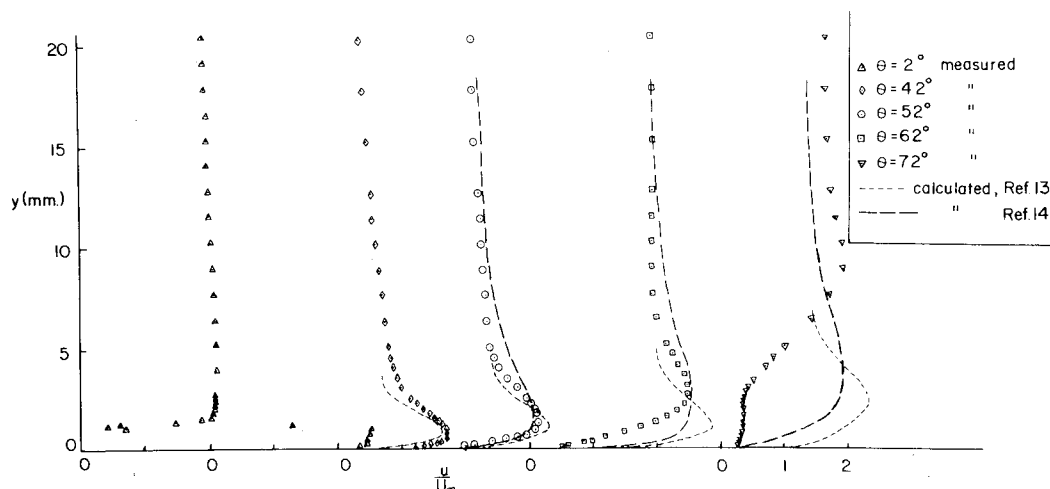


Fig. 9 Measured and calculated velocity profiles for flow D.



Figures 9-11 show the velocity profiles measured on the cylinder for flows D, E, and F. These profiles were measured at a spanwise position  $z = -1$  cm from the plane of symmetry, where the aforementioned spanwise fluctuations are relatively weak, as shown in Fig. 3. The upstream boundary layer on the cylinder develops over a short distance and in a strong favorable pressure gradient; it is therefore thin and is rapidly entrained into the wall jet. The velocity profiles and also the static pressure distributions in Fig. 5 clearly show that all of

these flows separate from the cylinder after traveling a relatively small distance from the injection slot. This is not surprising in view of the very strong and sustained adverse pressure gradient in the attached portion of the flow.

Flows A, B, and C are representative of the flow on a blown flap at moderate flap angles. In flows D, E, and F the upstream boundary layer is relatively thin, but in other respects these strongly curved flows are representative of flows downstream of the slot on circulation-controlled airfoils or at

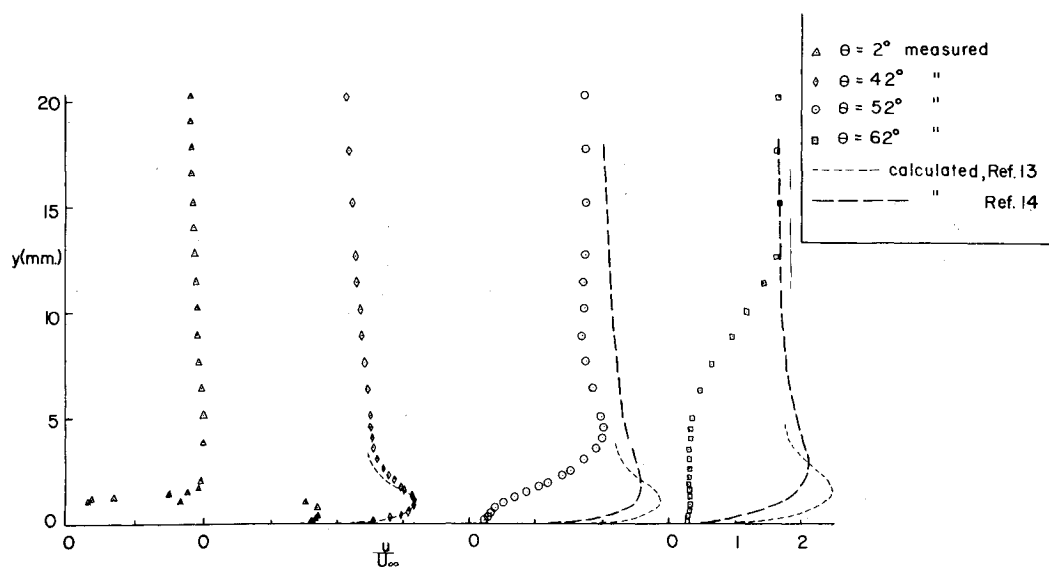


Fig. 10 Measured and calculated velocity profiles for flow E.

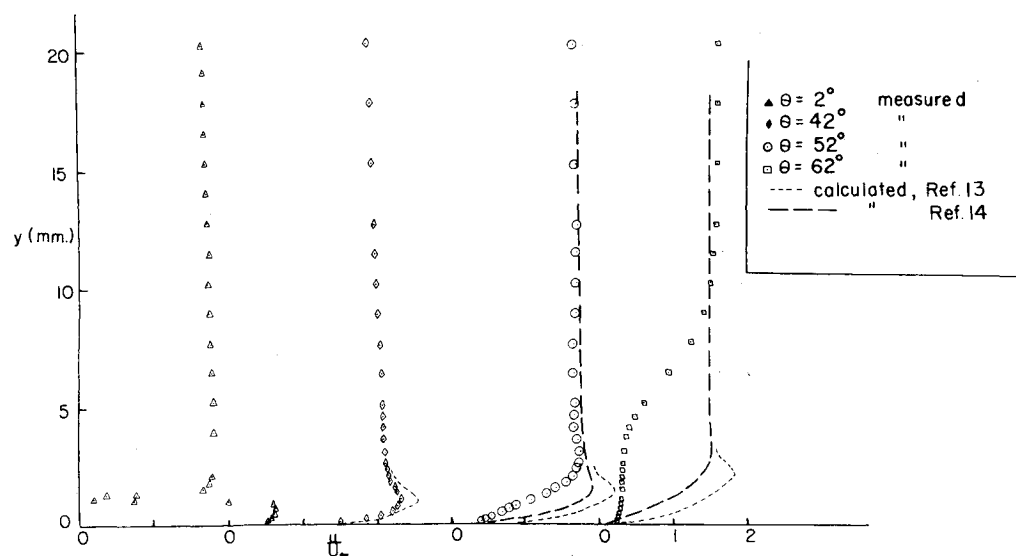


Fig. 11 Measured and calculated velocity profiles for flow F.

the knee of highly deflected blown flaps. The strong convex curvature in these flows has two important effects. It gives rise to a substantial variation of static pressure normal to the surface, as shown in Fig. 5; thus the pressure gradients along the curved wall are quite different from those at the outer edge of the shear layer, and this can be expected to have an important influence on flow separation. Furthermore, the radial gradient of angular momentum is negative in the outer region of the wall jet on the cylinder. This portion of the flow is therefore unstable and mixing with the external flow is much more rapid than in the case of a plane wall jet. This has the desirable consequence that the fluid from the upstream boundary layer is entrained relatively rapidly, thus minimizing the risk that a velocity minimum will persist and deepen, eventually causing the external flow to separate from the wall jet. An undesirable consequence of rapid mixing, on the other hand, is relatively rapid decay of the maximum velocity in the wall jet; this results in relatively early separation of the flow from the surface as observed in flows D, E, and F.

### C. Comparison with Prediction Methods

Included in Figs. 6-11 are velocity profiles calculated using two different prediction methods.<sup>13,14</sup> So far as the authors are aware, these methods are the most recent ones claiming the ability to predict strongly curved flows with tangential injection.

The method of Ref. 13 is an integral method which uses four parameters to describe the velocity profiles. The four unknown profile parameters are determined by applying the integral momentum equation to four different layers of the flow. Eddy viscosity correlations are used to determine the shear stresses at the edges of the layers. The calculation only extends out as far as the outer edge of the wall jet, and no attempt is made to predict the velocity profiles beyond that point. Incompressible flow is assumed.

The method of Ref. 14 is a finite-difference method and thus has much greater flexibility in representing the complex and varied velocity profile shapes encountered in flows with tangential injection. This method also uses an eddy viscosity model to establish shear stresses in the flow. This is less sophisticated than some of the closure assumptions currently being used to model the Reynolds shear stress behavior. It does, however, mean that the method is still fast enough to allow routine uses in the iterative computational schemes (e.g., Ref. 17) required to calculate the performance of circulation-controlled airfoils and airfoils with blown flaps.

The integral method was started using a "slot start" routine built into the method. The finite-difference method was started using the first velocity profile measured downstream of the slot.

The velocity profiles calculated by both methods agree quite well with those measured on the plane wall, when the profiles have a distinct velocity maximum and are not close to

Table 2 Separation positions

Flow	Measured separation position, deg	Predicted separation position, deg	
		Ref. 13	Ref. 14
D	$\theta = 75$	76	72.6
E	$\theta = 68$	74	64.1
F	$\theta = 63$	63	59.4

separation (Figs. 6 and 7). The finite-difference method continues to perform reasonably well when the measured profiles are tending to become like those of a conventional turbulent boundary layer as in Fig. 8, but here the integral method has difficulty in predicting the correct profile shape.

Both methods have considerable difficulty with the flows on the strongly curved wall (Figs. 9-11). The profiles well upstream of separation ( $\theta < 42$  deg) are reasonably well predicted, but as the flows approach separation ( $\theta > 52$  deg) the calculated profiles "hug" the wall to a much greater extent than the measured profiles. Nevertheless the finite-difference method does still give the correct general profile shapes and velocity maxima and is generally superior to the integral method in these difficult test cases.

The accuracy with which separation can be predicted is, of course, of particular interest. The measured and predicted separation positions are listed in Table 2. The measured positions are determined from the surface static pressure distributions of Fig. 5 by linearly extrapolating the pressure distribution somewhat upstream of separation to the constant wake pressure. The integral and finite-difference methods assume that separation occurs when the power-law exponent near the wall becomes  $\frac{1}{2}$  and when skin friction becomes zero, respectively. The separation positions are seen to be quite well predicted; in particular the trend given by the finite-difference method is good.

### Conclusions

Velocity profile measurements are presented for two-dimensional plane and highly curved flows with tangential injection, typical of flows on blown trailing edge flaps or at the trailing edge of circulation-controlled airfoils. Comparisons of the data with two prediction methods indicates that a useful prediction capability exists, but that improvements are desirable. In particular, difficulties are presented by flows near separation in strong adverse pressure gradients on highly curved surfaces. Additional flowfield data would be highly desirable to further assess capabilities of prediction methods and to guide efforts to improve them.

### Acknowledgment

This work received financial support from the National Research Council of Canada through Operating Grant A-5173.

### References

- Kind, R.J. and Maull, D.J., "An Experimental Investigation of a Low-Speed Circulation-Controlled Aerofoil," *Aeronautical Quarterly*, Vol. 19, May 1968, pp. 170-182.
- Williams, R.M., "Application of Circulation Control Rotor Technology to a Stopped Rotor Aircraft Design," *Vertica*, Vol. 1, Jan. 1976, pp. 3-15.
- Englar, R.J., Trobaugh, L.A., and Hemmerly, R.A., "STOL Potential of the Circulation Control Wing for High-Performance Aircraft," *Journal of Aircraft*, Vol. 15, March 1978, pp. 175-181.
- Kruka, V. and Eskinazi, A., "The Wall Jet in a Moving Stream," *Journal of Fluid Mechanics*, Vol. 20, Pt. 4, 1964, pp. 555-579.
- Kacker, S.C. and Whitelaw, J.H., "Some Properties of the Two-Dimensional Turbulent Wall Jet in a Moving Stream," *Journal of Applied Mechanics*, Vol. 35, Dec. 1968, pp. 641-651.
- Gartshore, I.S. and Newman, B.G., "The Turbulent Wall Jet in an Arbitrary Pressure Gradient," *Aeronautical Quarterly*, Vol. 20, Feb. 1969, pp. 25-56.
- Irwin, H.P.A.H., "Measurements in Blown Boundary Layers and Their Prediction by Reynolds Stress Modelling," Ph.D. thesis, McGill University, Montreal, Canada, 1974.
- McGahan, W.A., "The Incompressible Turbulent Wall Jet in an Adverse Pressure Gradient," Ph.D. thesis, MIT, Cambridge, Mass., 1965.
- Giles, J.A., Hays, A.P., and Sawyer, R.A., "Turbulent Wall Jets on Logarithmic Spiral Surfaces," *Aeronautical Quarterly*, Vol. 27, Aug. 1966, pp. 201-215.
- Wilson, D.J. and Goldstein, R.J., "Turbulent Wall Jets with Cylindrical Streamwise Curvature," *Journal of Fluids Engineering*, Vol. 98, Sept. 1976, pp. 550-557.
- Guittton, D.E. and Newman, B.G., "Self-Preserving Turbulent Wall Jets Over Convex Surfaces," *Journal of Fluid Mechanics*, Vol. 81, Pt. 1, 1977, pp. 155-185.
- Kind, R.J., "A Proposed Method of Circulation Control," Ph.D. dissertation, University of Cambridge, Cambridge, England, 1967.
- Kind, R.J., "A Calculation Method for Boundary Layer Control by Tangential Blowing," *Canadian Aeronautics and Space Institute Transactions*, Vol. 4, Sept. 1971, pp. 88-98.
- Dvorak, F.A., "Calculation of Turbulent Boundary Layers and Wall Jets over Curved Surfaces," *AIAA Journal*, Vol. 11, April 1973, pp. 517-524.
- Fekete, G.I., "Coanda Flow of a Two-Dimensional Wall Jet on the Outside of a Circular Cylinder," McGill University, Mechanical Engineering Research Labs., Rept. No. 63-11, 1963.
- Guittton, D.E., "Two-Dimensional Turbulent Wall Jets over Curved Surfaces," McGill University, Mechanical Engineering Research Labs., Rept. No. 64-7, 1964.
- Dvorak, F.A. and Kind, R.J., "An Analysis Method for the Viscous Flow Over Circulation-Controlled Airfoils," *Journal of Aircraft*, Vol. 16, Jan. 1979, pp. 23-29.